CO-PYROLYSIS OF E-WASTE AND BIOMASS FOR FUEL OIL PRODUCTION

Synopsis of the thesis to be submitted in the partial fulfilment of the award of the degree of

Doctor of philosophy

In

Chemical Engineering

PRAJAPATI SONALBEN BACHUBHAI
(Enrollment No: 189999911007)

Department of Chemical Engineering,
Government Engineering College,
Bhuj, Gujarat, India.

Under the supervision of
Dr. Shina Gautam
Associate Professor
Department of Chemical Engineering
Shroff S R Rotary Institute of Chemical Technology

Gujarat Technological University
Ahmedabad-382424, Gujarat, India
November 2022

1. Abstract

PCB, one of the main fractions of E-waste, is now becoming a source of pollution due to the presence of brominated flame retardants, which unleash highly toxic materials when burnt in presence of oxygen. Co-pyrolysis, which employs two or more feedstock together to transform solid waste into valuable solid, gas, and liquid while minimizing toxins, is one of the greatest solutions for reducing this waste. In the present research, cotton stalk (CS) as biomass was used in different composition with PCB, and its effects on chemical and physical characteristics of pyrolysis oils and char were evaluated, as well as possible reaction pathway of brominated epoxy resin of PCB and reduced toxicity in co-pyrolyzed products were derived. The slow pyrolysis of PCB, CS and co-pyrolysis with different compositions have been carried out in a fixed bed reactor, for temperature up to 500 ℃, and heating rate 10 $℃/min$. The Produced oil had been analysed in GC-MS and fuel properties of the oil measured as per FAME and compared. The generated gas was also analysed in GC. Moreover, the raw sample and char degradation behaviour was evaluated using Thermo-Gravimetric Analysis and Derivative Thermogravimetric Analysis (TGA/DTG) and the influence of co-pyrolysis process on chemical composition and physical attributes of the produced char as well as the advantages and effects of different CS ratio on product yield was determined. The physicochemical properties and morphological aspects of char were determined using a variety of analytical techniques, including nitrogen physisorption using the BET method, FE-SEM coupled with an EDS, FTIR, XRF and XRD. The most essential aspect of char analysis was bromine content, which was found to be increased with co-pyrolysis, showing that the co-pyrolysis process assisted in reducing bromine content in oil and fixing it in char.

Keywords: Co-Pyrolysis, TGA, PCB, Biomass, GC/MS, Fuel Properties

2. Background and definition of the Problem

The world is currently dealing with a number of environmental issues as a result of rapid growth in manufacturing activities, inappropriate management strategies, and existing waste management laws and regulations; more recently, e-waste has emerged as an emerging environmental issue as a result of short product life cycles and rapidly advancing technology in the province of EEE's (Electrical and Electronic Equipment), which has resulted in vast quantities of comparatively new electronic products being discarded, as a result, E-waste builds up three times quicker than other waste [1]. According to [2], 20 to 50 million tonnes of e-waste are produced globally each year [3], with India ranking first among the top five e-waste producers with an estimated yearly production of 2 million tonnes [4]. As per [5] in his recent research, globally, 53.6 Mt of e-waste were created in 2019, up 9.2 Mt from 2014, and it is anticipated to hit 74.7 Mt by 2030. This is the most serious matter for developing countries, which serve as a collection point for dumped material from developed countries and escalate the problem due to a lack of recycling infrastructure. As a necessity, developing countries such as Asia and Africa, for eg. India, Pakistan, China, Nepal, Bangladesh, Bhutan, Ghana and Nigeria must find environmentally acceptable ways to dispose of or recycle E-waste.

Printed circuit boards (PCBs), which are a heterogeneous mixture of organic materials, glass fibres and metals, make up around 3-6% of all electrical and electronic equipment, complicating the recycling process [6]. After mechanical separation of plastics and metals what remains behind is epoxy resin and this waste is just landfilled or incinerated causing release of toxic metals like Pb, Sn, Ca, Cu, Hg [7]. As per [8] PCBs are one of the major challenges in most electronic fractions, which are manufactured mainly with epoxy or phenol resin containing a fire retardant, such as tetra-bromo-bisphenol-A (TBBA). Some of the processes employed include mechanical dismantling to separate plastics and metals, as well as thermal recycling, hydrometallurgical and pyrometallurgical facilities, leaching, and amalgamation to recover valuable metals [9]. However, there was no separation of plastics with brominated flame retardants and the leftover PCBs were just landfilled or incinerated. Landfilling of the brominated chemicals, like their chlorinated congeners, may pose serious effect on plants, soil, water and microbial species found in the nearby area; whereas, incineration produces a high quantity of toxic polycyclic aromatic hydrocarbons (PAH), polyhalogenated aromatic hydrocarbons (PHAH) as well as PBDD/F (Poly-bromo dibenzodioxines/furans), PCDD/F (Poly-chlorodibenzodioxines/furans) and HBr with brominated phenols as by-products [10][11][12] which is catalytically amplified by the presence of heavy metals, especially copper and its oxides [13]. It pollutes air, ultimately contaminate our food chain and adversely affect to humans' skin, liver, and digestive tract. A number of studies have been carried out about the toxicity and the health risks concerning the human exposure in TBBA (tetrabromobisphenol-A) on recycling sites [14][5][15]. Therefore, environmentally acceptable disposal or recycling of waste PCB which can replace conventional traditional procedures with futuristic state of the art eco-friendly approaches is a big challenge [10][16]. By adopting more appropriate processing conditions during recycling, it is feasible to minimise the amount to which they are generated. Furthermore, it is need of the environment to find a simple, effective, and optional solution to increase the energy security of a nation, achieve effective waste management, and reduce dependency on fossil fuels [17].

1.2 Motivation and Definition of the Problem

Pyrolysis of PCB has been demonstrated in several studies to be an effective waste valorisation approach to address the issues stated above [11][18]. It allows large polymer chains of PCBs to be broken up into lighter polymer compounds with smaller molecular weight. Slow pyrolysis (Temperature ~ 500 ℃ , hot vapor residence time ~ 2 sec, and very fast condensation to prevent the scope of secondary reactions) on the other hand, produces the maximum amount of oil while also producing solid char and gases [19][20]. The amount of oil, solid char, and gas produced are mainly influenced by the temperature, raw material and hot vapour residence time with many other factors like additives, catalysts and technology [21]. The produced liquid oil can be hydro deoxygenated into fuels for automobile engines, fed into boilers alone or in combination with fossil fuels, or even employed as a more suitable resource of H_2 than biomass [13][22]. Conversely, this is only appropriate if the pyrolysis products have low halogen yields [23]. In fact, dehalogenation of oil products is one of the most important aspects of pyrolysis treatment. In this context, co-pyrolysis (a process which involves two or more different

materials as feedstock) could be an alternative technology that improves these two criteria. Co-pyrolysis of biomass has been shown in several studies to boost oil yield and quality while maintaining the overall process. Furthermore, biomass is renewable and underutilised in energy conversion technologies, and has been identified as a possible energy source owing to its low sulphur and nitrogen content [21]. A high amount of hydrogen present in biomass may lead to dehalogenation and prevention of PBDD/F which promotes HBr / HCl fixation in char [24]. Furthermore, the biomass has a higher H/C molar ratio than PCBs which can act as a hydrogen donor to PCBs during co-pyrolysis. Water, one of the most abundant components in biomass, is expected to act as a reactive agent, promoting further cracking of the PCBs tar and the production of more volatile chemicals, hence improving pyrolysis oil yields; However, the product yields and characteristics are influenced by the temperature, residence time and blend ratio of the two feedstocks [25]. Moreover, because of the various reactivities of biomass and PCBs, this process is relatively complex.

In this work, Cotton Stalk (CS) as biomass was used because of its many benefits; Cotton is one of the most widely cultivated crops in Gujarat, India. Following cotton removal, the remaining cotton stalks are considered as waste and are simply burned to dispose of them, harming the environment. While characterization studies of cotton stalks suggest that it contained a high amount of volatile matter and a low O/C ratio which can aid in improving the quality and quantity of bio-oil.

3. Objectives and scope of work

- To understand pyrolysis behaviour (such as initial degradation temperatures, thermal degradation rates, and residual weight) of PCB, CS and its mixture at different CS:PCB compositions by TGA/DTG analysis.
- To find pyrolysis kinetics of the main thermal decomposition processes and identify possible reaction mechanisms.
- To study oil characterization using GC/MS and find possible reaction pathways for the debromination.
- To find the fuel characteristics of generated oil using FAME standards, and its potential applications. Moreover, application of generated gas is also explored.
- To compare the morphological and physical characteristics of the co-pyrolyzed CS:PCB char, as well as its potential applications.

4. Original Contribution of the research

Based on the background information previously covered, the current study sheds light on the slow pyrolysis of PCB and CS and was compared with the co-pyrolysis of different CS and PCB compositions on a lab scale fixed bed reactor, and the synergistic effect was assessed. This research examines the impact of different CS compositions on co-pyrolysis products in order to obtain lower halogen yields and limiting toxic emissions while achieving increasing oil yield. Moreover, potential applications for pyrolysis oil, gas and char are explored. The

present investigation also includes the comparison for morphological and physical attributes of co-pyrolyzed char with PCB, and CS char, including pore size distribution, surface area, porosity, structural properties, and elemental analysis. Most importantly, bromine content in char with respect to increased CS composition is evaluated.

As per the authors best knowledge, there was no single literature that focused on the thermal decomposition and co-pyrolysis of these residues. Its compositions might be the first expanding research effort to understand the synergistic behaviour of the mixture. Additionally, there are various studies available in literature on individual behaviour of PCB and Cotton Stalk pyrolysis, however, co-pyrolysis of the both and its product characterization has been evaluated first time from authors best knowledge.

5. Methodology of research

5.1 Sample Preparation

The PCB used in this analysis was obtained from Shiwalik solid waste management located at Punjab, where epoxy resin was already separated from metals and crushed through hammer mill to get 100-200 μm average particle size of epoxy resin. The CS samples, on the other hand, were collected from a local farm in Gandhinagar, Gujarat-India, and were air-dried, crushed and sieved to acquire the same particle size as PCB then mixed to ensure homogenous distribution by divide and mix technique.

5.2 TGA Analysis

TGA and DTG were conducted using Mettler Toledo equipment. The furnace temperature was set at 700 ℃ and approximately 10 mg of sample was heated from ambient to 700 ℃ at heating rate 10 $℃/min$ using N_2 as inert gas with flow rate 50 *ml/min*. The same parameters were used in pyrolysis experiments.

5.3 Pyrolysis experiments

A SS 316 fixed bed cylindrical reactor, see **Fig. 1**, was used to carry out pyrolysis experiments with a 100 mm ID (inner diameter), height of 320 mm and 7 mm thickness, surrounded by three parallel electrical heaters each of 2 kW and appropriately insulated with glass wool. The top of the reactor was open from where 200 g of the sample was fed for each experiment. Nitrogen was purged through silica frit from the reactor bottom and the reactor temperature raised from ambient to 500 ℃. As the temperature increased, the feed vapours evolved and passed through glass condenser connected to a chiller which is maintained at 2 ± 0.1 ℃ temperature. Finally, generated liquid, gas and solid char were collected and their corresponding percentages were calculated.

5.4 Sample Analysis

Chemical composition of the pyrolysis oil was determined using GC-MS (Gas chromatography–mass spectrometry) analyser by Thermo Scientific TSQ 8000 equipment, and collected gas samples were analysed by gas chromatography with model Shimadzu GC-2014.

Additionally, oil samples were also analysed according to FAME standards to determine its fuel characteristics.

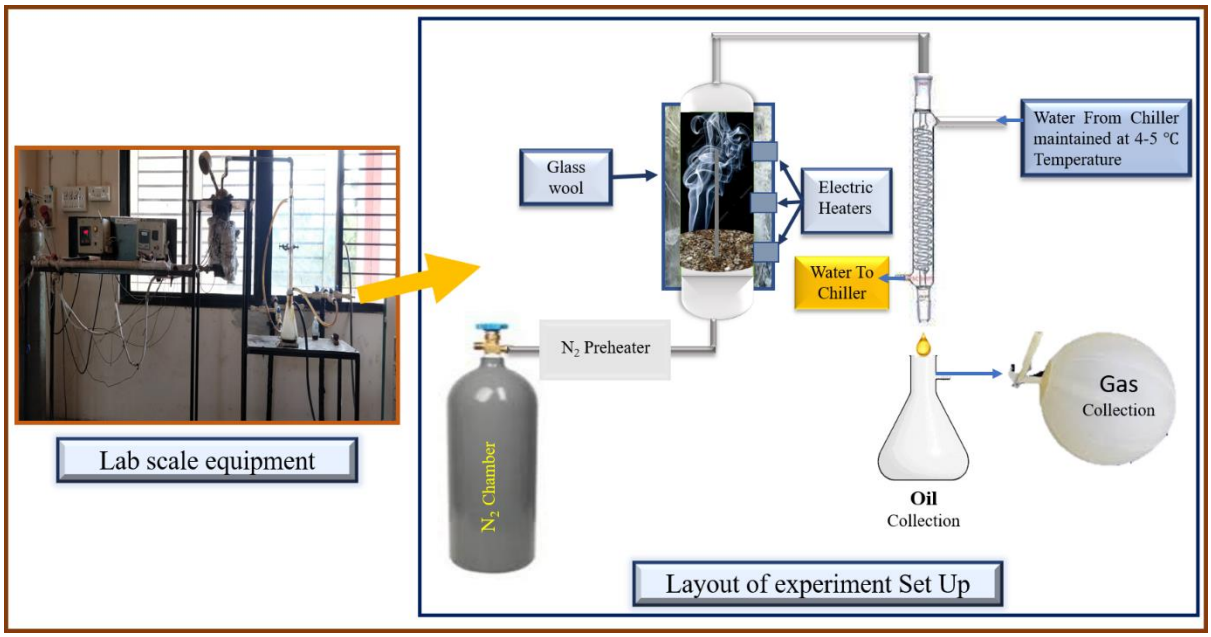

Figure 1: Lab scale equipment with layout of experimental setup.

Moreover, several characterization techniques were utilized to examine and determine the char attributes, such as TGA/DTG was performed using N_2 as inert gas on Mettler Toledo with 10 °C*/min* heating rate, heated from ambient temperature to 1000 °C. The physicochemical properties and morphological aspects of char were determined using a variety of analytical techniques, including nitrogen physisorption using the Brunauer-Emmet- Teller (BET) method, Field Emission Scanning Electron Microscope (FE-SEM) coupled with an X-ray energy dispersive system spectroscopy (EDS), Fourier transform infrared (FTIR), X-ray fluorescence spectroscopy (XRF) and X-Ray Diffraction (XRD).

6. Results and Discussion

6.1 Thermal Analysis (TGA/DTG)

The thermal degradation of PCB, CS, and different CS:PCB composition is depicted in **Fig. 2 (a)**. The mass loss percent in the diagram reflects the solid residual mass fraction, which can be a mixture of non-reacted solids and residue formed. The mass loss region formed before 100 ºC for CS was due to the vaporization of moisture and vitrification transition, whereas in PCB it attributed to depolymerisation, which resulted in release of water and low molecular weight aliphatic and aromatic hydrocarbons such as CO_2, HBr, and CH_3COCH_3. The emergence of the shoulder in the DTG curve could be attributed to hemicellulose and cellulose degradation in the CS sample and tetra-bromo-bisphenol-A degradation in the PCB sample. Whereas, a constant slow deterioration corresponds to the degradation behaviour of lignin in CS and the breakage of ether bonds in brominated resin in PCB, which results in bisphenol A, propyl alcohol and/or small phenolic molecules.

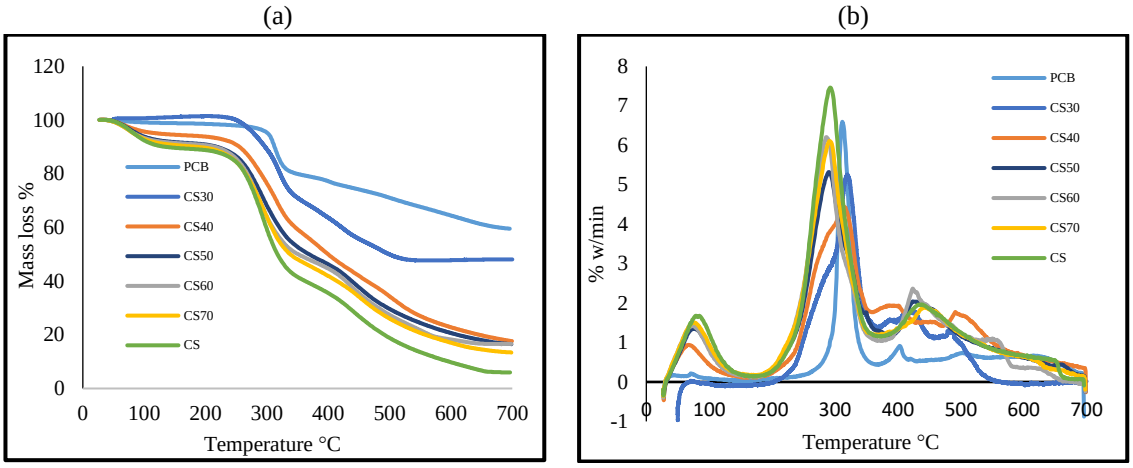

Figure 2: TGA and DTG plots as a function of temperature at heating rates of 10 ℃/min.

As illustrated in DTG curve **Fig. 2(b)** the pyrolysis reflected a peak at 200-370 ℃, with a maximum degradation temperature (T_m) at 293 ℃ for CS and 302 ℃ for PCB. However, the maximum degradation peak for different CS:PCB compositions shift left hand side with increasing amount of CS and lies between 293-324 ℃. A steady degradation of second stage was occurred between 370 and 600 °C and devolatilization was not found for all samples, indicating char formation and a carbonization stage. Furthermore, **Table 1** indicates the amount of mass lost at each stage, as well as the residue in % mass. As an outcome with increased amount of biomass, the residue percentage falls, allowing volatiles to rise and hence increasing the oil yield.

Table 1: % of mass loss at each stage and % residue for the samples.

Sample	Actual Mass loss %	De-moisturisation Mass loss %	Char Generation Mass loss %	Overall Mass loss %	Residue %
PCB	32	1.5	6.5	40	60
CS	77	11	6	94	6
CS30	52	0	0	52	48
CS40	69	6	7	82	18
CS50	70	8	6	84	16
CS60	72	9	3	84	16
CS70	72	10	5	87	13

6.2 Proximate and Ultimate Analysis of the sample

Table 2 shows general characteristics and elemental analysis for different feedstock. As the amount of CS in the sample was increased from 30 to 70%, the O/C molar ratio increased from 0.86 for CS30 to 1.56 for CS70, implying that biomass had a lower energy density than PCB[26][26][24]. Additionally, the total organic matter (C, H, O) of the PCB was 39.88%, while for a mixture, it was increased with increased CS concentration ranging from 69.72% for CS30 to 73.49% wt/wt for the CS70. On the other hand, H/C ratio was highest with CS70. This higher H/C ratio as well as lower ash content and fixed carbon could be the reason for the slightly increase in calorific value of CS70.

Table 2: General characterisation and elemental analysis of raw feedstock.

Sample	HCV MJ/kg	Proximate Analysis				Ultimate Analysis						H/C	O/C
		Moisture %	Ash (%)	Volatile Material (%)	Fixed C (%)	C (%)	H (%)	N (%)	S (%)	O (%)	Others* (%)		
PCB	10.55	14.05	43.95	41.87	0.13	26.73	2.39	1.93	0.19	10.76	58.00	0.09	0.40
CS	11.24	23.93	5.49	70.51	0.07	32.52	4.12	2.15	0.16	31.63	29.42	0.13	0.97
CS30	11.31	3.35	24.34	62.22	10.09	35.60	3.34	2.55	0.04	30.78	27.69	0.09	0.86
CS40	10.58	4.12	23.48	68.32	4.08	29.96	4.76	1.95	0.12	35.61	27.60	0.16	1.19
CS50	11.12	5.20	23.73	68.20	2.87	28.76	5.45	2.86	0.15	35.85	26.93	0.19	1.25
CS60	10.76	6.88	19.75	71.27	2.10	26.07	6.15	2.34	0.39	38.41	26.64	0.24	1.47
CS70	12.15	8.28	16.03	72.58	3.11	25.79	7.41	2.08	0.11	40.29	24.32	0.29	1.56

*Others calculated from difference of ultimate analysis (C, H, N, S and O).

6.3 Kinetic Analysis

6.3.1 Determination of apparent activation energy

The primary goal of this study is to comprehend the thermal degrading behaviour of PCB and CS and to compare it to various CS:PCB compositions. For this, a TGA study is conducted at three different heating rates (5, 10, and 15 °C/min) in a nitrogen environment, and the apparent activation energy (E_α) and pre-exponential factor (A) were calculated using the Kissinger Akahira Sunnose (KAS) (Eq. 1), Flynn-Wall- Ozawa (FWO) (Eq. 2), and Starink (Eq. 3) were calculated according to Eq. (1), (2) and (3) respectively.

$$ln\left(\frac{\beta}{T^2}\right) = ln\left(\frac{AE}{Rg(\alpha)}\right) - \frac{E}{RT} \quad (1)$$

$$ln\beta = ln\frac{AE}{Rg(\alpha)} - 5.331 - 1.052\frac{E}{RT} \quad (2)$$

$$ln\left(\frac{\beta}{T^{1.8}}\right) = ln\left(\frac{AE}{Rg(\alpha)}\right) - 1.0037\frac{E}{RT} \quad (3)$$

To determine the kinetic parameters, we chose the same value of α ranging from 0.2 to 0.9 during the major thermal decomposition process, at different heating. Finally, a Criado differential-integral master plot was used to identify relevant decomposition mechanisms.

From the results, R^2 values for all the samples with FWO method, were higher than KAS and Starink, so activation energy based on FWO method only reported here, See **Table 3** and **Table 4**.

6.3.2 Determination of the most probable reaction model

The reference theoretical curves, known as "master plots," have been used in many research that have analysed experimental data [27]. A method to ascertain the samples' reaction mechanism at a fixed heating rate was put out by Criado et al.[27]. It employs the concept of

Table 3: Activation energy obtained by FWO model-free methods for PCB, CS and different compositions at First zone.

α	PCB		CS		CS30		CS40		CS50		CS60		CS70	
	E (KJ/mol)	R^2	E (KJ/mol)	R^2	**E (KJ/mol)**	**R^2**	**E (KJ/mol)**	**R^2**	**E (KJ/mol)**	**R^2**	**E (KJ/mol)**	**R^2**	**E (KJ/mol)**	**R^2**
0.1	166.57	0.5989	105.91	0.9122	120.08	0.9961	97.74	0.8951	132.90	0.9923	179.77	0.9837	437.41	0.9924
0.2	190.21	0.7923	121.43	0.9422	181.77	0.9987	116.87	0.9514	151.60	0.9932	170.39	0.9736	280.85	0.996
0.3	169.06	0.9743	130.82	0.9658	131.1	0.9008	133.35	0.9612	154.67	0.9825	157.35	0.9709	233.91	0.9983
0.4	144.06	0.9932	132.70	0.9731	149.75	0.9989	171.17	0.9759	162.78	0.985	151.39	0.9402	212.13	0.9865
0.5	133.38	0.9991	141.12	0.9681	150.51	0.9986	176.28	0.9754	157.08	0.9582	149.41	0.9416	219.13	0.9998
0.6	123.94	0.9968	137.16	0.9726	137.69	0.9644	162.92	0.993	144.69	0.9978	139.13	0.9514	200.9	0.9931
0.7	115.02	0.9927	138.51	0.9897	123	0.9531	144.1	0.9988	137.56	0.97	138.84	0.977	196.19	0.9937
0.8	96.43	0.9517	143.95	0.9945	115.56	0.9979	130.04	0.9968	117.64	0.8829	157.49	0.9998	209.41	0.988
0.9	93.89	0.9432	151.88	0.9546	115.42	0.9867	115.12	0.9936	105.67	0.7687	143.44	0.9905	228.52	0.9114
Avg. (0.1-0.9)	136.95		133.72		136.1		138.62		140.51		154.13		246.49	
Avg. (0.2-0.9)	138.87		135.10		138.1		143.73		146.57		150.93		222.63	

Table 4: Activation energy obtained by FWO model-free methods for PCB, CS and different compositions at Second zone.

α	PCB		CS		CS30		CS40		CS50		CS60		CS70	
	E (KJ/mol)	R^2	E (KJ/mol)	R^2	**E (KJ/mol)**	**R^2**	**E (KJ/mol)**	**R^2**	**E (KJ/mol)**	**R^2**	**E (KJ/mol)**	**R^2**	**E (KJ/mol)**	**R^2**
0.1	-677.80	0.8838	153.04	0.9647	108.37	0.9461	144.08	0.9997	96.07	0.6956	74.2	0.9885	111.18	0.9687
0.2	-181.41	0.9473	197.06	0.9654	117.66	0.9948	137.36	0.982	113.07	0.9493	69.22	0.9922	146.76	0.9997
0.3	-113.42	0.978	179.78	0.9446	105.29	0.9946	114.48	0.9951	114.38	0.9227	69.13	0.9668	132.06	0.9863
0.4	-85.21	0.8767	152.92	0.9388	98.14	0.9953	101.33	0.9688	125.65	0.9453	77.03	0.971	120.17	0.9999
0.5	-80.66	0.7933	140.65	0.9435	105.42	0.9978	134.59	0.956	170.68	0.9975	86.49	0.9918	124.59	0.965
0.6	-89.37	0.7518	117.64	0.9288	102.13	0.9995	146.89	0.9427	185.59	0.9743	102.78	0.9927	81.24	0.9792
0.7	-110.03	0.7648	98.01	0.9025	91	0.9902	133.51	0.9811	214.51	0.9691	94.21	0.9866	63.93	0.992
0.8	-217.77	0.7472	88.96	0.9001	73.18	0.9949	119.87	0.9965	230.15	0.9993	83.88	0.9824	51.73	0.9961
0.9	-553.81	0.6932	79.23	0.8841	59.16	0.9978	95.26	0.9822	275.07	0.924	66.99	0.992	63.94	0.998
Avg. (0.1-0.9)	-234.39		134.14		95.6		125.26		169.46		80.44		99.51	
Avg. (0.2-0.9)	-125.41		139.29		94		122.91		164.86		81.22		98.05	

reduced time plots, proposed by Ozawa [27] for α against t/ tα , where tα is the time to reach a certain value of α (usually 0.5 to 0.9). Here, 10 °C/min heating rate was randomly selected.

Theoretical curve: $$\frac{Z(\alpha)}{Z(0.5)} = \frac{f(\alpha)g(\alpha)}{f(0.5)g(0.5)} \quad (4)$$

Experimental curve (Master curve): $$\frac{Z(\alpha)}{Z(0.5)} = \left(\frac{T_\alpha}{T_{0.5}}\right)^2 \frac{(d\alpha|dt)_\alpha}{(d\alpha|dt)_{0.5}} \quad (5)$$

Plotting the graph of $\frac{Z(\alpha)}{Z(0.5)}$ vs α for different mechanisms, theoretical curves were obtained. By using known value of activation energies, the experimental $\frac{Z(\alpha)}{Z(0.5)}$ value were derived and overlapped to check best match of the reaction mechanism. In Figure 3, only CS70 sample is shown for reference.

The acquired experimental curve, for the second zone of all four samples, is highly equivalent to the m13 mechanism of **Table 5**. While, for the first zone, CS60 demonstrates the m13 mechanism, CS30 exhibits the m12, and CS40 exhibits the m11 reaction mechanism. Importantly, the CS70 for the first zone demonstrates two distinct reaction mechanisms, m11 for α = 0.2–0.5 and m13 for α = 0.2–0.5.

6.3.3 Kinetic compensation effects

For any solid-state decomposition, the kinetic parameters, specifically the pre-exponential factor *A* and the activation energy *E*, exhibit the following relationship:

$$ln\, A = aE + b \quad (6)$$

where, *a* and *b* are constants and refer to the compensation coefficients.

Above equation represents linear relation between *In A* and *E* for a series of related reactions or for the same reaction carried out in a series of different conditions, known as a compensation effect. In fact, the compensating effect offers a potential way to anticipate how experimental conditions would affect kinetic parameters.

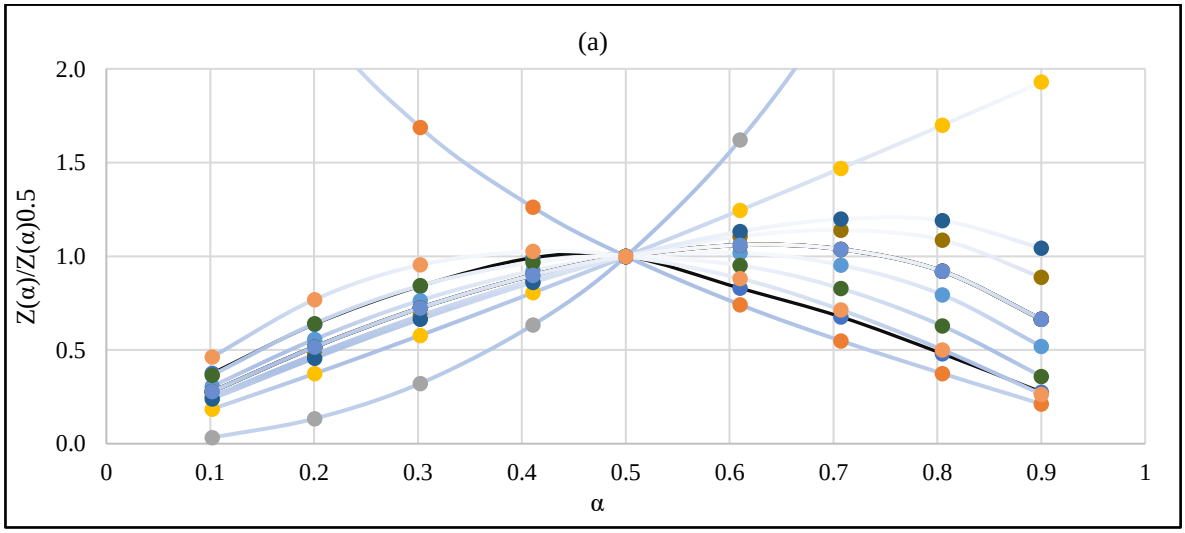

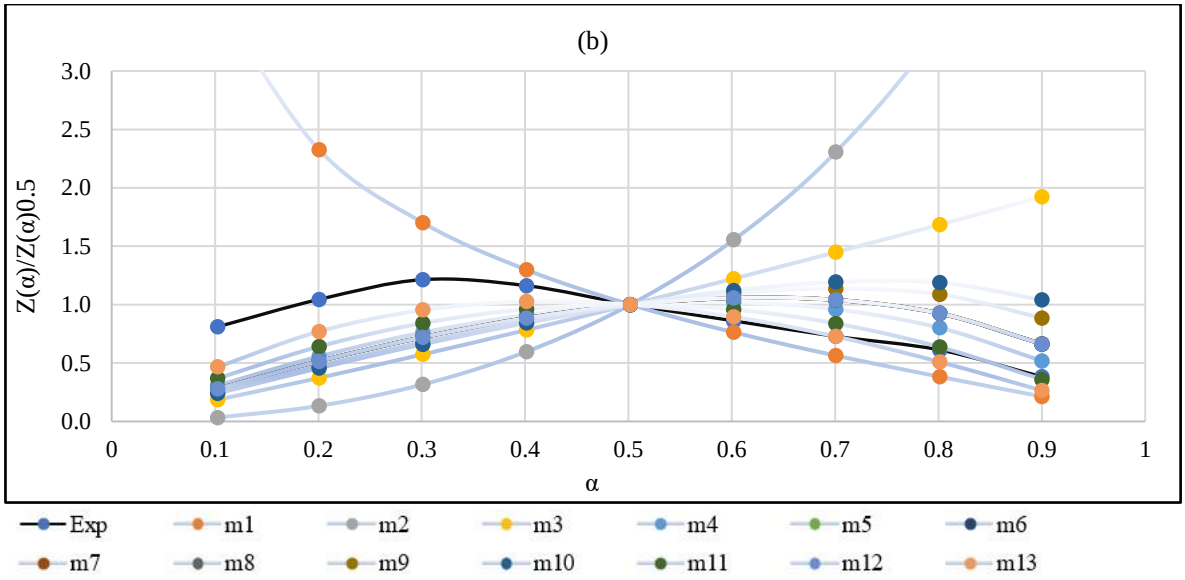

Figure 3: Criado plots of CS70 for first zone (a) and second zone (b).

Table 6 displays the value of the pre-exponential factor in the form of *ln A*, obtained by substituting E_α and $g(\alpha)$ values in Eq. (2). The $g(\alpha)$ values were determined based on approximated reaction mechanism by Criado master plots.

Table 5: Different degradation mechanisms with f(α) and g(α).

No.	Function name	Mechanisms	f(α)	g(α)
m1	Jander equation	Diffusion, 3D (spherical symmetry)	$3/2(1-\alpha)^{2/3}[1-(1-\alpha)^{1/3}]^{-1}$	$[1-(1-\alpha)^{1/3}]^{1/2}$
m2	G–B equation	Diffusion, 3D (column symmetry)	$3/2[(1-\alpha)^{-1/3}-1]^{-1}$	$1-2\alpha/3-(1-\alpha)^{2/3}$
m3	Anti–Jander equation	Diffusion, 3D	$3/2(1+\alpha)^{2/3}[(1+\alpha)^{1/3}-1]^{-1}$	$[(1+\alpha)^{1/3}-1]^2$
m4	Z–L–T equation	Diffusion, 3D	$3/2(1-\alpha)^{4/3}[(1-\alpha)^{-1/3}-1]^{-1}$	$[(1-\alpha)^{-1/3}-1]^2$
m5	Avrami–Erofeev Equation	Random nucleation and nuclei growth, n=3	$3(1-\alpha)[-\ln(1-\alpha)]^{2/3}$	$[-\ln(1-\alpha)]^{1/3}$
m6	Avrami–Erofeev Equation	Random nucleation and nuclei growth, n=2	$2(1-\alpha)[-\ln(1-\alpha)]^{1/2}$	$[-\ln(1-\alpha)]^{1/2}$
m7	Avrami–Erofeev Equation	Random nucleation and nuclei growth, n=3/2	$3/2(1-\alpha)[-\ln(1-\alpha)]^{1/3}$	$[-\ln(1-\alpha)]^{2/3}$
m8	Avrami–Erofeev Equation	Random nucleation and nuclei growth, n=4/3	$4/3(1-\alpha)[-\ln(1-\alpha)]^{1/4}$	$[-\ln(1-\alpha)]^{3/4}$
m9	Geometrical contraction	Shrinkage geometric shape ((column symmetry)	$3(1-\alpha)^{2/3}$	$1-(1-\alpha)^{1/3}$
m10	Geometrical contraction	Shrinkage geometric shape, (spherical symmetry)	$2(1-\alpha)^{1/2}$	$1-(1-\alpha)^{1/2}$
m11	Reaction order n=2	Chemical reaction	$(1-\alpha)^2$	$(1-\alpha)^{-1}-1$
m12	Reaction order n=1	Chemical reaction	$(1-\alpha)$	$-\mathrm{Ln}(1-\alpha)$
m13	Reaction order n=3	Chemical reaction	$(1-\alpha)^3$	$((1-\alpha)^{-2}-1)/2$

Table 6: Pre-exponential factor derived using FWO method.

Conversion (α)	First Zone (lnA)					Second Zone (lnA)				
	CS30	CS40	CS50	CS60	CS70	CS30	CS40	CS50	CS60	CS70

0.2	33.81	18.8	27.00	31.35	57.04	13.42	11.15	12.54	4.9	10.66
0.3	21.84	22.36	27.50	28.24	45.47	11.24	10.83	12.85	4.82	10.5
0.4	25.7	30.63	29.21	27.28	40.15	10.03	9.37	14.80	6.19	9.25
0.5	25.6	31.49	27.88	27.02	41.32	11.2	9.38	22.24	8.36	8.5
0.6	22.67	28.36	25.20	24.91	37.57	10.72	8.64	24.47	11.14	7.61
0.7	19.43	24.36	23.87	24.23	36.43	9.16	7.38	28.99	9.96	5.13
0.8	17.75	21.54	20.20	28.42	39.28	6.93	6.96	31.42	8.78	3.91
0.9	17.48	18.79	18.67	26.15	43.52	5.99	7.1	38.52	7.27	4.69
Avg (0.2-0.9)	22.68	24.54	24.94	27.2	42.6	9.84	8.85	23.23	7.68	7.53

6.4 Pyrolysis Experiments

Pyrolysis for all samples were performed on the lab scale set up, as discussed above. Each sample ran for 3 times to replicate the results due to heterogeneous nature of the samples. As per TGA analysis discussed above the optimum temperature for producing maximum oil was in the range of 200 - 500 °C. Above 500 ℃, secondary reactions took place and more volatiles from char could come out in the form of gas. Whereas too low temperature can cause incomplete decomposition of the biomass [10][28].

6.4.1 Effect of different composition on product yield

Fig. 4(a) shows that for PCB, the amount of oil is lowest (19.6%) and the amount of char is highest (59.6%); however, for CS the contrary is evident with the highest oil (36%) and lowest char (28%). Furthermore, because of containing more volatile components and moisture, amount of oil generated by co-pyrolysis rose significantly as CS was increased, reaching at peak at CS70 (31.5%). Similarly, the amount of gas produced increased dramatically with increasing CS up to 60 % then somewhat drops with 70 % CS (see **Fig. 4(b)**), owing to the fact that numerous large hydrocarbon molecules had been broken into smaller molecules [29][30][31]. Furthermore, as the amount of CS increases, the amount of char created falls dramatically until it reached a plateau for 70% CS.

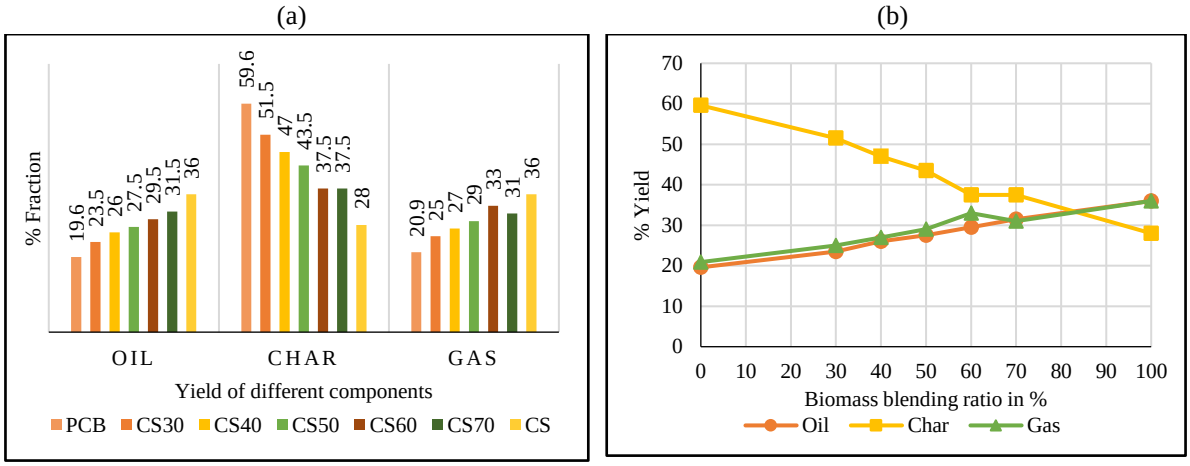

Figure 4: (a) Comparison of % fraction generated in each sample, (b) Yield of the different sample with different biomass blending ratio.

6.4.2 Liquid oil characterisation

The GC-MS analysis of the collected oil was used to determine the nature and type of components present without breaking them down. More than 25 unique aromatic and aliphatic compounds were found in each sample during first 40 minutes of GC-MS spectra acquisition, however the compounds with an area percent of more than 0.1 are discussed here. The % of a compound in the oil was equivalent to the area percent of the peak for that component.

Table 7: The amount of phenol and phenolic compounds identified in each sample, as % area.

Compound name	% Area						
	PCB	CS	CS30	CS40	CS50	CS60	CS70
phenol	38.47	21.85	56.74	48.28	54.83	55.21	55.78
2-methyl, phenol	5.07	-	8.42	6.76	5.04	6.4	6.92
4-methyl, Phenol	5.66	3.73	3.9	5.94	3.77	3.35	5.5
phenol, 2,3-dimethyl	-	-	-	-	2.36	-	-
Phenol, 2-ethyl	0.28	-	-	-	0.3	-	-
phenol, 3,4-dimethyl-	2.54	0.36	2.14	2.92	1.62	2.01	2.6
Phenol, 3,4,5-trimethyl-	-	-	1.01	0.85	0.54	0.93	0.7
phenol, 3-(1-methylethyl)	4.31	-	4.58	4.12	6.17	5.97	2.8
Phenol, m-tert-butyl-	-	-	-	-	0.88	-	-
P-isopropenylphenol	2.94	-	1.84	-	1.31	1.42	-
phenol, 4-ethyl	1.4	-	-	0.9	-	-	-
Total	60.67	25.94	78.63	69.77	76.82	75.29	74.3

*phenolic compounds in the order CS30>CS50>CS60>CS70>CS40.

The GC-MS analysis revealed that the major products of PCB and its compositional pyrolysis oil were fragments of the polycarbonate epoxy resin, with phenol being the most abundant component. They tend to form between 450 - 500 °C, however their quantity decreases as the temperature rises above 500 °C, due to secondary reactions that may further decompose it in smaller molecules.

Table 7 describes the value of phenol and phenolic compounds identified in PCB, CS, and different CS:PCB combinations. PCB had total of 60.67% phenol and phenolic compounds, while CS had just 25.94%. It can be attributed to the combined effect of bisphenol A decomposition in epoxy resin of PCB and lignin decomposition of CS. It is to be pointed out that in the presence of biomass, pyrolysis of polycarbonate (Bisphenol A) can lead to an increased phenolic compounds in the oil [30]. The order of highest phenol and phenolic compounds were found for different CS composition in the order: CS30>CS50>CS60>CS70>CS40, see **Table 7**.

Table 8 indicates the list of compounds found in the different CS:PCB compositions, excluding phenol and phenolics, and the concentration is compared with 100% PCB and CS samples. Those compounds are classified based on some of the functional groups which involved alkyne, ketone, ester, siloxane, nitrile, furan, pyridyl, PAHs and phosphate ester.

6.5 Debromination and other hydrocarbons removal of oil

Slow pyrolysis of PCB with CS was facilitated elimination of bisphenol A completely as no traces were found in pyrolysis oils. Also, no bromine compounds were found except ethanone,1(3-bromo-4-hydroxyphenyl) in PCB oil with a very small amount (0.16 % area) and

it was totally removed or below detection limit in co-pyrolysis products. Indicating, in the present study, biomass acts as a hydrogen donor in the debromination reaction and the increased supply of hydrogen in the phenol resin aids in the conversion of most organic bromine to inorganic HBr and its fixation in char.

Table 8: Compound found other than phenol and phenolics, based on functional groups.

Functional Group	Compound Name	% Area						
		PCB	CS30	CS40	CS50	CS60	CS70	CS
Alkyne	Benzene,1-ethynyl-4-methyl	1.3	0.15	0.77	-	0.25	0.81	-
	4,6-octadiyn-3-one, 2-methyl	-	1.4	3.27	-	-	2.17	-
ketone	2-pentanone, 4-hydroxy-4-methyl	-	0.4	0.5	-	0.73	0.79	5.44
	Ethanone, 1-(2,3-dihydro-1H-inden-5-yl)-	-	0.57	0.5	0.22	0.32	0.09	-
	5',6',7',8'-Tetrahydro-2'-acetonaphthone	0.6	0.75	0.6	0.98	0.79	0.26	-
	Methanone, (2-methylphenyl)phenyl-	0.3	0.18	0.27	0.16	0.14	0.08	-
Ester	Pentadecanoic acid, 14-methyl-, methyl ester	-	0.2	0.3	0.28	0.37	0.14	1.07
Siloxane	Cyclotetrasiloxane, octamethyl-	0.5	0.24	0.14	0.18	0.18	0.13	-
Nitrile	Benzonitrile	-	1.73	-	-	1.71	1.14	-
	Pentadecanenitrile	0.1	0.09	0.08	0.23	0.15	0.03	-
Furan	Benzofuran, 2-isopropenyl-3-methyl-	0.4	0.41	0.43	0.42	0.35	0.16	-
	Dibenzofuran	0.8	0.29	0.55	0.36	0.26	0.18	-
Pyridyl	1h-pyrrolo[2,3-b]pyridine,1-methyl-	4.6	3.62	3.38	-	2.54	3.03	-
PAHs	Acenaphthylene	0.4	0.11	0.31	0.12	0.1	0.13	-
	Fluorene	0.4	0.28	0.45	0.4	0.44	0.19	-
	Anthracene	1	0.23	0.64	0.23	0.16	0.21	-
	Fluoranthene	0.2	0.13	0.21	0.13	0.15	0.09	-
	Naphthalene	4	1.8	2.58	1.89	1.96	2.91	-
	Naphthalene, 2-methyl-	1.1	0.67	0.87	-	-	0.4	-
	Naphthalene, 2-ethenyl	0.9	0.26	0.37	0.31	0.23	0.15	-
Phosphate ester	Triphenyl phosphate	0.2	0.29	0.36	0.2	0.21	0.14	-

*4,6-octadiyn-3-one, 2-methyl is fall under alkyne and ketone functional groups. *2-pentanone, 4-hydroxy-4-methyl falls under ketone and alcohol group.

Furthermore, as shown with the GC/MS data, none of the oil samples contained PBDD/Fs (product of TBBA fire retardant in presence of oxygen), attributable to the reductive environment of the pyrolysis process, which makes the formation of de-hydrogen or de-hydroxyl radicals impossible.

6.6 Gas Analysis

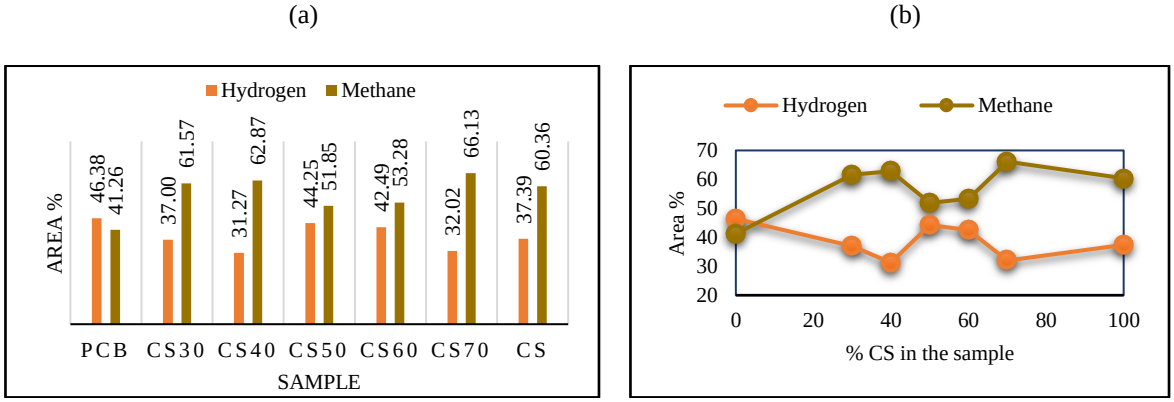

Figure 5: (a) amount of gas produced in % area, (b) Comparison chart of effect of CS composition on gas yield.

Gas Chromatogram indicated H_2 and CH_4 as the most abundant pyrolysis gas in all the samples. Whereas, a very small amount of other hydrocarbons like C_2H_6 and C_2H_4 were also detected.

We can deduce from the results, (See, **Fig. 5**) that using a 70% CS in PCB can increase the quantity of methane, which is one of the key fuels in industries, but using a 50:50 CS:PCB composition can maximise the amount of hydrogen in gas. There were no indications of halogen gases, which is a positive result because hydrogen halides are extremely corrosive and can cause the development of dioxins and furans when used as fuel.

6.7 Physical Properties of generated oil

Pyrolysis oil of PCB, CS, and various CS:PCB compositions were tested using FAME (Fatty acid methyl esters) test methods, which was used to define the product to be used as automotive diesel fuel. Different parameters were compared with automotive diesel fuel Bharat Stage VI (IS 1460-2017), as shown in **Table 9**. The results revealed that all quality parameters of the pyrolysis oils did not meet the IS automotive diesel fuel and FAME criteria, with the exception of CS50. However, CS50 also did not followed the phosphorous content and calorific value (28.41 MJ/kg). Most importantly, bromine content in PCB oil was found to be 77 mg/100 g of sample, whereas, it decreased in pyrolysis oils with increasing CS amount; in CS70 oil it was found to be lowest (18.18 mg/100 g).

Table 9: Fuel properties of the pyrolyzed oil samples, compared with automotive diesel fuel and FAME standards.

Test Parameters	Unit	PCB	CS	CS30	CS40	CS50	CS60	CS70	Bharat stage VI (IS 1460-2017)	FAME Limits
Density 15°C	g/cm³	0.912	0.923	0.915	0.908	0.88	0.911	0.903	0.815-0.845	0.86-0.9
Kinematic Viscosity @ 40 °C	mm²/s	4.4	4.46	5.12	4.95	4.11	5.25	4.26	2.0-4.5	3.5-5
Distillation	%@ °C	90%	93%	94%	85%	95%	92%	79%	-	-
Flashpoint	°C	120	123	122	119	126	114	114	66 @ 40°C	Min. 101
CFPP	°C	45	43	48	45	45	51	40	6 °C winter, 18 °C summer	-
Cloud point	°C	-31	-29	-32	-29	-32	-30	-27	-	-
Sulphur	mg/kg	18	15	19	28	8	30	23	Max10	Max. 10
CCR 100%	%mass	19	16	22	18	18	26	15	-	-
Carbon residue (10 % dist.residue)	%mass	0.56	0.4	0.55	0.52	0.22	0.49	0.47	0.3	Max.0.30
Sulphated ash	%mass	0.067	0.056	0.045	0.056	0.012	0.032	0.04	-	Max. 0.02
Oxid ash	%mass	0.33	0.25	0.61	0.34	0.14	0.54	0.26	-	-
Water	mg/kg	840	852	829	831	413	824	827	Max. 200	Max 500
Total contamination	mg/kg	32	29	28	31	24	25	28	max. 24	24
Cu corrosion	3h/50°C	1	1	1	1	1	1	1	Not worse than No.1	class 1
Oxidation stability	hrs;110°C	6 hours	6 hours	6 hours	6 hours	6 hours	6 hours	6 hours	-	Min. 6 hours
Cetane number		47	49	53	48	51	56	44	Min. 51	Min. 51
Acid value	mgKOH	0.45	0.38	0.52	0.4	0.43	0.43	0.36	0.2	0.5

C(x:4) & greater unsaturated esters	%mass	1	1	1	1	1	1	1	-	Max. 1
Phosphorus	mg/kg	18	15	31	28	10	28	31	-	4
PAHs	%mass	0.25	0.32	0.35	0.52	0.42	0.18	0.2	Max. 8	-
Lubricity/ wear	µm at 60 °C	15	8	12	16	10	9	13	Max. 460	-
Bromine Content	mg of Br_2 per 100 gm of sample	77.53	48.41	43.47	32.88	28.1	22.45	18.18	-	-
Calorific value	MJ/kg	23.16	24.19	25.16	22.45	28.41	26.52	20.95	43-46 [31][32][33]	-

6.8 Characterization of CS:PCB char

6.8.1 Proximate Ultimate analysis of char

An ultimate and proximate analysis of CS and PCB and different mixtures are shown in **Table 10**. It can be seen that hydrogen concentration for various compositions of CS:PCB char samples decreased with increasing biomass concentration in comparison to PCB, while the carbon content was increased. Moreover, oxygen content of CS50 and CS70 is much lesser. This suggests that hydrogen and oxygen are lost at a faster rate than carbon in these co-pyrolyzed char. The PCB sample had a larger loss on drying (LOD) than the CS sample, which can be related to dehydration response of water content as well as release of more volatile components such as CO_2, CO, and CH_4.

Table 10: Proximate and ultimate analysis of the char sample.

Properties	PCB	CS	CS30	CS40	CS50	CS60	CS70
Proximate analysis (wt. %)							
LOD	4.41	0.92	1.12	2.03	1.26	1.14	1.19
Ash	68.59	8.96	75.15	79.13	78.71	64.92	78.76
VM	16.51	56.69	21.25	17.99	18.9	22.29	19.04
Fixed Carbon (%)	10.49	33.43	2.48	0.85	1.13	11.65	1.1
Ultimate Analysis (wt %)							
Hydrogen	1.89	2.51	0.96	0.85	0.71	1.98	0.47
Carbon	23.87	23.1	32.71	55.91	82.5	32.12	88.17
Nitrogen	1.32	4.52	1.58	1.85	1.12	2.44	1.18
Sulphur	0.074	0.605	0.174	0.17	0.287	0.277	0.304
Oxygen	31.44	16.19	47.06	22.51	10.09	46.24	7.62
Others*	41.406	53.075	17.516	18.71	5.293	16.943	2.256
HHV(MJ/Kg)	5.13	8.51	3.96	16.08	27.11	5.38	29.12
H/C	0.08	0.11	0.03	0.02	0.01	0.06	0.01
O/C	1.32	0.70	1.44	0.40	0.12	1.44	0.09

*Others calculated from difference of ultimate analysis (C, H, N, S, O).

The ash content of PCB char was 68.59% consisted incombustible inorganic material, was increased with co-pyrolysis and highest value was achieved for CS40 (79.13 %). This higher ash content of co-pyrolysis char may be the reason of thermal breakdown of organic molecules, resulting in CO_2 emission and formation and condensation of mineral elements [34].

In comparison to other compositions, CS70 has a high quantity of fixed carbon, total carbon, lower H/C ratio and higher HHV (29.45 MJ/Kg), as well as a reduced level of ash content, indicating that removing the ash from CS70 char could lead to its use as a solid fuel. Furthermore, fuels with lower H/C and O/C ratio as CS70, is highly favourable due to lower smoke generation, water vapor production and loss of energy during combustion. The highest amount of C (88.17 %) and lowest amount of O (7.62 %) of CS70, could make it useful for operations such as removing contaminants from aqueous matrices.

6.8.2 TGA Analysis of char

TGA **Fig. 6(a)** and DTG **Fig. 6(b)** curves show endothermic heat effects for different char samples. The samples were heated from ambient to 1000 ℃ in an inert atmosphere with 10 $℃/min$. A very slow and initial weight loss was visible up to 150 ℃ for PCB and co-pyrolyzed samples, the reason may be release of moisture and smaller molecules. The same behaviour was attributed to CS sample before 120 ℃, after that no apparent change in the sample weight was observed up to 400 °C. The high rate of decomposition for PCB, CS and the mixture char began about 370 °C, whereas for the mixture CP50 it started around 320 °C. The maximum rate of breakdown for PCB char was occurred close to 540 °C, followed by very gradual and continuous mass loss, whereas the highest rate of decomposition for the CS and mixtures occurred above 500 °C, associated with degradation of cellulose followed by hemicellulose degradation and above 800 - 900 °C the minor decomposition was associated with lignin decomposition. The co-pyrolysis most likely resulted in a stable carbon form that can endure higher temperatures, hence improved thermal stability.

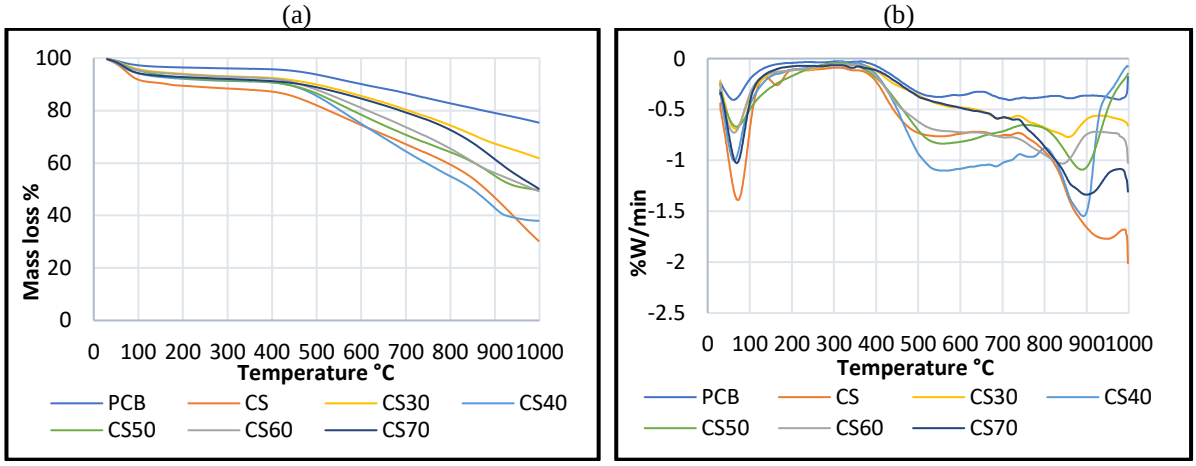

Figure 6: (a) TGA curves and (b) DTG curves obtained in an inert atmosphere at 10 $℃/min$ heating rate for PCB and cotton stalk and CS:PCB mixture

Moreover, **Fig. 6(a)** shows that the overall mass loss for PCB was 25% explaining high ash content. For CS it was found 70%. However, the overall mass loss for co-pyrolyzed char sample for CS30 was 38%, whereas it was around 50% for CS50, CS60, and CS70 and was highest at CS40 (62%). This observation indicated that CS30 char took longer to decompose and more thermally stable structure than other compositions at the same operating temperature and heating rate.

6.8.3 Surface area and porosity

The primary surface properties of all char samples were determined using BET analysis (**Table 11**). The samples exhibited an average pore diameter of 2 to 50 nm, indicating that they were mesoporous materials filled by capillary condensation.

Table 11: BET surface area and porosity of the char samples.

Sample	Average pore diameter (nm)	BET Surface area (m^2/g)	Total pore volume (cm^3/g)
PCB	3.458	2.575	0.005
CS	25.604	4.535	0.024
CS30	3.475	16.791	0.027
CS40	3.484	3.187	0.006
CS50	3.507	0.736	0.002
CS60	3.484	2.913	0.006
CS70	3.485	6.226	0.011

It's worth noting that capillary condensation implies, filling of residual pore space left after multilayer adsorption with the condensate which is separated from the gas phase by menisci. CS30 had a significantly high surface area (16.791 m^2/g) indicating a higher adsorption capacity than other co-pyrolyzed char samples. However, other samples either PCB or CS or the mixture had lower surface area due to persistent volatile materials causing co-pyrolyzed char porosity to be blocked, indicating very low reactivity.

6.8.4 FE-SEM and EDS analysis

FESEM pictures of chars generated in a fixed bed reactor are shown in **Fig. 7(a-h)**. All chars revealed the existence of tiny particles and pores, with a rough texture, a heterogeneous surface, and a diversity of randomly distributed pore sizes. The FESEM image of PCB char **Fig. 7(a)** shows the presence of a number of metals (Cu, Sn, Zn etc.) as bright spots and carbon as dark regions. CS shown in **Fig. 7 (c)** consisted of large particles with a smooth surface, whereas, small globular vesicle formation has been seen in CS30 char during char formation **Fig. 7 (d)**. Lignin particles melted and released volatile materials, leading in the production of open pores on the particle with rough surface and irregular outlet, resulting in a significantly increased surface area. However, if volatiles are not completely diffused out, larger vesicles are generated and stick to the surface, which can lead to pore blockage. Water permeation into the pores is another cause of pore blockage, which diminishes surface area.

According to Sharma et al. [35], alkali metal K enrichment of cotton stalk char can cause agglomeration and even severe devolatilization, and plastic transformation may occur due to solid matrix softening and cell structure melting, resulting in pore closure. However, increased CS ratios, such as CS40 and above, **Fig. 7 (e-h)**, could result in the strengthening of the degradation reaction and forceful release of gaseous substances that did not entirely diffuse out and then condensed during the cooling process, resulting in the generation of more twisted agglomerated and rough vesicles.

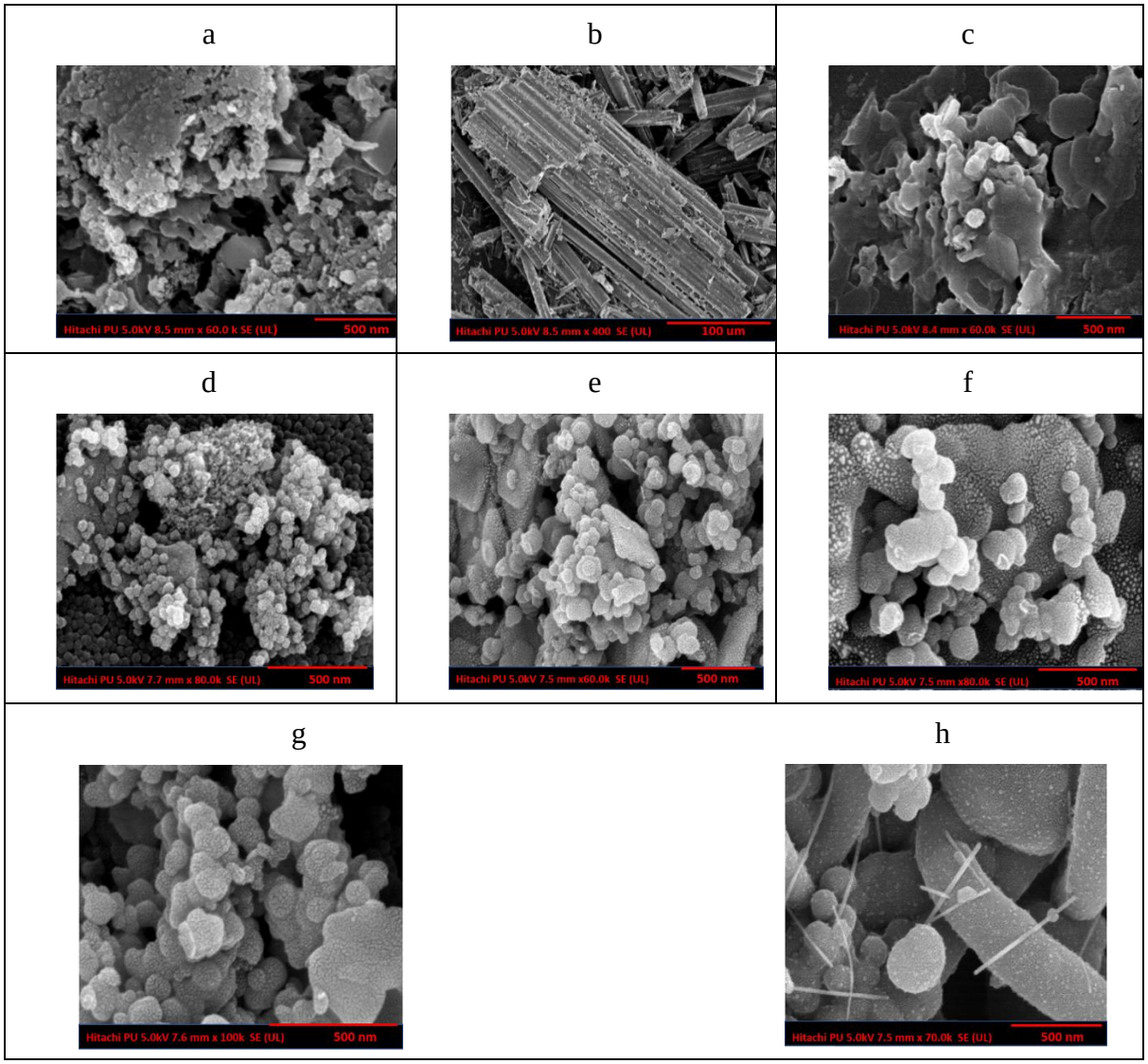

Figure 7: FESEM micrographs of (a) 500 nm resolution PCB char (b) 100 nm resolution PCB char, (c) CS, (d) CS30, (e) CS40, (f) CS50, (g) CS60 and (h) CS70 at 500 nm resolution

EDS examination verified the existence of nonmetal-inorganic elements like Si and Ca from ceramic and glass fibre, as well as metals like Al, Fe. Oxygen was also present which can contribute to develop slag oxides (Al_2O_3, Fe_2O_3, SiO_2, etc.) and can be seen as light grey patches. Additionally, the presence of N, C, Mg, K, Ca, Fe, S, and P are nutrient components for plant growth [36], and the increased C elements are an indicator of condensed aromatic rings, which are likely to stick with soils.

Table 12: % of mineral content present in each sample by FESEM-EDS

	K	S	Al	Si	Ca	Fe	N	P	Mg	Cl
PCB	-	-	4.88	14.13	10.71	1.77	2.24	0.69	0.27	-
CS	19.33	4.53	-	-	-	-	1.68	1.35	0.05	0.76
CS30	0.2	0.18	5.01	13.8	4.9	0.06	2.83	0.17	0.55	0.08
CS40	1.08	0.14	10.36	5.51	2	0.19	-	-	0.09	1.35
CS50	0.9	-	-	-	-	-	3.2	1.85	0.35	-
CS60	0.44	0.09	2.89	7.01	5.53	0.93	3.86	0.13	0.15	0.26
CS70	0.74	0.24	0.18	1.09	0.06	0.52	-	0.37	0.03	0.02

6.8.5 X-ray Fluorescence Analyses

XRF (X-ray Fluorescence) analysis was done to determine the principal metals and other elements quantity. The bromine content in PCB char is the source of brominated fire retardants in epoxy resins, which is due to CS as the hydrogen donor assisted in the release of brominated compound in the form of HBr and its fixation in char. As shown in **Fig. 8**, Br content was 32% in PCB char and 31.8% in CS char, which increased in co-pyrolyzed chars with elevated biomass. The chlorine content in PCB was very less 0.5 % which was increased to maximum 2.41% with CS70. Also, Pb concentration was increased from 0.7% in PCB to 1.93% in co-pyrolyzed CS30 char. Phosphate was also present in PCB char (0.41%) due to phosphate-based fire retardants and concentration in char had slightly increased with co-pyrolysis to maximum 1.3 % for CS70. Many other metals like, barium, sulphur, aluminium and manganese were also present as shown in **Fig. 8**.

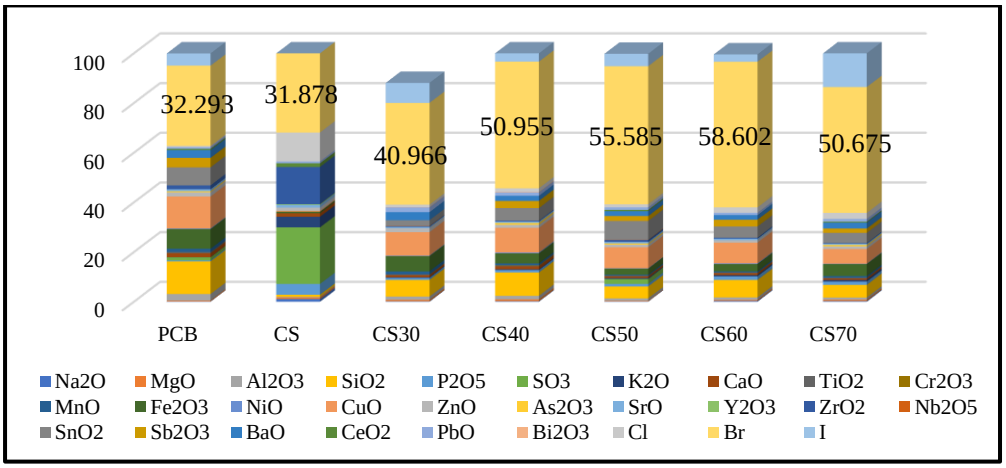

Figure 8: XRF analysis data comparison of metals oxides and other elements like bromine present in all char samples

7. Achievements with respect to objectives

To understand pyrolysis behaviour (such as initial degradation temperatures, thermal degradation rates, and residual weight) of PCB, CS and its mixture at different CS:PCB compositions by TGA/DTG analysis.	TGA/DTG analysis was made to find the thermal degradation rate, residual weight and maximum degradation temperature of each sample.
To find pyrolysis kinetics of the main thermal decomposition processes and identify possible reaction mechanisms.	Three non-isothermal, iso-conversional methods KAS, FWO and Starink were applied to find Kinetic triplets and Criado method was applied to see the probable reaction mechanism.
To study oil characterization using GC/MS and find possible reaction pathways.	Lab scale fixed bed co-pyrolysis experiment was made and the produced oil was characterised by GC/MS and possible

	reaction pathways for the debromination and the improved phenolic compounds were figured out.
To find the fuel characteristics of generated oil using FAME standards, and its potential applications.	Fuel characteristics of the produced oil from different CS:PCB compositions were examined and compared. Moreover, probable applications of generated oil and gas were explored.
To compare the morphological and physical characteristics of the co-pyrolyzed CS:PCB char, as well as its potential applications.	The morphological and physical characteristics of the co-pyrolyzed CS:PCB chars were found by BET, FESEM-EDS, FTIR, N_2 adsorption-desorption, XRF and XRD analysis.

8. Conclusion

This work employed a lab-scale co-pyrolysis experiments, in order to increase oil quality and quantity while reducing brominated compounds, using a variety of CS:PCB compositions (CS30, CS40, CS50, CS60, and CS70) and comparison was done by their physical and chemical characterisation. PCB had total of 60.67 % phenol and phenolic compounds, while CS had just 25.94 %. However, as CS composition was increased during co-pyrolysis, the amount of phenol and phenolic compounds were increased and with CS50 the highest amount (78.63 %) of phenol and phenolic compounds were observed.

The advantage of using cotton stock with PCB was, it acted as a hydrogen donor in the debromination reaction and aided in conversion of most organic bromine to inorganic HBr and its fixation in char. A CS70 composition showed an increase in methane in generated gas which is one of the most essential fuels in industry, whereas a CS50 composition showed an increase in the amount of hydrogen. Oil from CS50 composition met all FAME parameters except for phosphorous concentration (10 mg/kg) and calorific value (28.41 MJ/Kg) to be used as a fuel. Further investigations are required into upgrading fuel oil, which may entail hydrodeoxygenation, catalytic cracking, and steam reforming.

Moreover, the influence of increasing amount of CS with PCB was found to be very effective in changing the morphology and texture of the char produced. In case of PCB pyrolysis, char yield was 60%, however, with co-pyrolysis amount was reduced due to CS early deterioration and char secondary decomposition at higher temperatures. TGA observation indicated that CS30 char took longer to decompose and more thermally stable structure than other compositions at the same operating temperature and heating rate. It also had more micro pores as well as larger pore volumes near 200 nm size range and has a surface area of 16.791 m^2/g, indicating a significantly higher adsorption capacity than other co-pyrolyzed char samples. However, it still needs to be activated before it can be used for sorption. In same sample

compositions small globular vesicle formation were observed during char formation, resulting in a significantly increased surface area.

As per proximate, ultimate analysis, CS70 has highest amount of C (88.17 %) and lowest amount of O (7.62 %) higher heating value (29.12 MJ/kg), as well as a reduced level of ash content which could make it useful for operations such as removing contaminants from aqueous matrices. Additionally, other indecisive applications of the created chars were also reliant on the existence of nutritional components and their physicochemical properties, which could only be taken into account once the bromine content was removed, which might be the future focus of the new research.

9. Future scope of work

CS50 fulfils all oil fuel FAME/ Bharat VI criteria except calorific value, however, adopting relatively simple processes like solvent addition to lower viscosity and chemical stability, filtration to remove char and alkali, bio-oil can be upgraded to meet the same quality standards. One of the direct applications for bio-oil is emulsification with diesel. Other upgrading technologies could also be applied, like Hydrodeoxygenation, catalytic cracking, and steam reforming of bio-oils, which are all extremely complicated procedures that require reliable and fully developed reactors.

CS30 char having higher BET surface area, which can further be improved by adopting reliable process to be used as adsorber in different applications.

CS70 has good calorific value and acceptable solid fuel properties, but it needs to be bromine free before using it as a solid fuel. So, the most important future scope is to find the economical, acceptable bromine removal techniques for solid char.

References:

[1] F. Cucchiella, I. D'Adamo, S.C. Lenny Koh, P. Rosa, Recycling of WEEEs: An economic assessment of present and future e-waste streams, Renew. Sustain. Energy Rev. 51 (2015) 263–272. https://doi.org/10.1016/j.rser.2015.06.010.

[2] Z. Wang, B. Zhang, D. Guan, Take responsibility for electronic-waste disposal, Nature. 536 (2016) 23–25. https://doi.org/10.1038/536023a.

[3] A. Kumar, M. Holuszko, D.C.R. Espinosa, E-waste: An overview on generation, collection, legislation and recycling practices, Resour. Conserv. Recycl. 122 (2017) 32–42. https://doi.org/10.1016/j.resconrec.2017.01.018.

[4] R.M.R. Turaga, K. Bhaskar, S. Sinha, D. Hinchliffe, M. Hemkhaus, R. Arora, S. Chatterjee, D.S. Khetriwal, V. Radulovic, P. Singhal, H. Sharma, E-Waste Management in India: Issues and Strategies, Vikalpa. 44 (2019) 127–162. https://doi.org/10.1177/0256090919880655.

[5] Ankit, L. Saha, V. Kumar, J. Tiwari, Sweta, S. Rawat, J. Singh, K. Bauddh, Electronic waste and their leachates impact on human health and environment: Global ecological threat and management, Environ. Technol. Innov. 24 (2021) 102049. https://doi.org/10.1016/j.eti.2021.102049.

[6] Q. Wang, B. Zhang, S. Yu, J. Xiong, Z. Yao, B. Hu, J. Yan, Waste-Printed Circuit Board Recycling: Focusing on Preparing Polymer Composites and Geopolymers, ACS Omega. 5 (2020) 17850–17856. https://doi.org/10.1021/acsomega.0c01884.

[7] N. Raje, E -Waste: Characterization and Disposal through Solid State Route, Int. J. Environ. Sci. Nat. Resour. 23 (2020) 33–43. https://doi.org/10.19080/ijesnr.2020.23.556106.

[8] C. Rosenberg, M. Hämeilä, J. Tornaeus, K. Säkkinen, K. Puttonen, A. Korpi, M. Kiilunen, M. Linnainmaa, A. Hesso, Exposure to flame retardants in electronics recycling sites, Ann. Occup. Hyg. 55 (2011) 658–665. https://doi.org/10.1093/annhyg/mer033.

[9] S. Salhofer, E-waste collection and treatment options: A comparison of approaches in Europe, China and Vietnam, Handb. Environ. Chem. 63 (2018) 227. https://doi.org/10.1007/698_2017_36.

[10] C. Quan, A. Li, N. Gao, Research on pyrolysis of PCB waste with TG-FTIR and Py-GC/MS, J. Therm. Anal. Calorim. 110 (2012) 1463–1470. https://doi.org/10.1007/s10973-011-2048-x.

[11] Y. Kim, S. Kim, J. Lee, Y. Park, Pyrolysis Reaction Pathways of Waste Epoxy-Printed Circuit Board 1,2, 30 (2013) 706–712. https://doi.org/10.1089/ees.2013.0166.

[12] Z. Yao, J. Xiong, S. Yu, W. Su, W. Wu, J. Tang, D. Wu, Kinetic study on the slow pyrolysis of nonmetal fraction of waste printed circuit boards (NMF-WPCBs), Waste Manag. Res. (2020). https://doi.org/10.1177/0734242X19896630.

[13] P. Evangelopoulos, E. Kantarelis, W. Yang, Investigation of the thermal decomposition of printed circuit boards (PCBs) via thermogravimetric analysis (TGA) and analytical pyrolysis (Py-GC/MS), J. Anal. Appl. Pyrolysis. 115 (2015) 337–343. https://doi.org/10.1016/j.jaap.2015.08.012.

[14] A. Sepúlveda, M. Schluep, F.G. Renaud, M. Streicher, R. Kuehr, C. Hagelüken, A.C. Gerecke, A review of the environmental fate and effects of hazardous substances released from electrical and electronic equipments during recycling: Examples from China and India, Environ. Impact Assess. Rev. 30 (2010) 28–41. https://doi.org/10.1016/j.eiar.2009.04.001.

[15] N. Singh, H. Duan, O.A. Ogunseitan, J. Li, Y. Tang, Toxicity trends in E-Waste: A comparative analysis of metals in discarded mobile phones, J. Hazard. Mater. 380 (2019) 120898. https://doi.org/10.1016/j.jhazmat.2019.120898.

[16] T.R. Mankhand, K.K. Singh, S.K. Gupta, S. Das, Pyrolysis of Printed Circuit Boards, 1 (2012) 102–107. https://doi.org/10.5923/j.ijmee.20120106.01.

[17] B.B. Uzoejinwa, X. He, S. Wang, A. El-Fatah Abomohra, Y. Hu, Q. Wang, Co-pyrolysis of biomass and waste plastics as a thermochemical conversion technology for high-grade biofuel production: Recent progress and future directions elsewhere worldwide, Energy Convers. Manag. 163 (2018) 468–492. https://doi.org/10.1016/j.enconman.2018.02.004.

[18] C. Quan, A. Li, N. Gao, Combustion and Pyrolysis of Electronic Waste : Thermogravimetric Analysis and Kinetic Model, Procedia Environ. Sci. 18 (2013) 776–782. https://doi.org/10.1016/j.proenv.2013.04.104.

[19] T. Bridgwater, Challenges and opportunities in fast pyrolysis of biomass: Part I, Johnson Matthey Technol. Rev. 62 (2018) 118–130. https://doi.org/10.1595/205651318X696693.

[20] M.N. Islam, M.H.M. Ali, M. Haziq, Fixed bed pyrolysis of biomass solid waste for bio-oil, AIP Conf. Proc. 1875 (2017). https://doi.org/10.1063/1.4998369.

[21] S.A. El-Sayed, M.E. Mostafa, Pyrolysis characteristics and kinetic parameters determination of biomass fuel powders by differential thermal gravimetric analysis (TGA/DTG), Energy Convers. Manag. 85 (2014) 165–172. https://doi.org/10.1016/j.enconman.2014.05.068.

[22] F.J. Sánchez-Borrego, P. Álvarez-Mateos, J.F. García-Martín, Biodiesel and Other Value-Added Products from Bio-Oil Obtained from Agrifood Waste, Processes. 9 (2021) 797. https://doi.org/10.3390/pr9050797.

[23] P. Hense, K. Reh, M. Franke, J. Aigner, A. Hornung, A. Contin, Pyrolysis of waste electrical and electronic equipment (WEEE) for recovering metals and energy: Previous achievements and current approaches, Environ. Eng. Manag. J. 14 (2015) 1637–1647. https://doi.org/10.30638/eemj.2015.175.

[24] F. Abnisa, W.M.A. Wan Daud, A review on co-pyrolysis of biomass: An optional technique to obtain a high-grade pyrolysis oil, Energy Convers. Manag. 87 (2014) 71–85. https://doi.org/10.1016/j.enconman.2014.07.007.

[25] Y. Shen, R. Yuan, X. Chen, X. Ge, M. Chen, Co-pyrolysis of E-waste Non-metallic Residues with Bio-wastes Co-pyrolysis of E-waste Non-metallic Residues with Bio-wastes, (2018). https://doi.org/10.1021/acssuschemeng.8b01439.

[26] W.J. Liu, K. Tian, H. Jiang, X.S. Zhang, G.X. Yang, Preparation of liquid chemical feedstocks by co-pyrolysis of electronic waste and biomass without formation of polybrominated dibenzo-p-dioxins, Bioresour. Technol. 128 (2013) 1–7. https://doi.org/10.1016/j.biortech.2012.10.160.

[27] J.M. Criado, J. Morales, Thermal decomposition reactions of solids controlled by diffusion and phase-boundary processes: possible misinterpretation of the mechanism from thermogravimetric data, Thermochim. Acta. 19 (1977) 305–317. https://doi.org/10.1016/0040-6031(77)80006-3.

[28] A.E. Pütün, N. Özbay, E.P. Önal, E. Pütün, Fixed-bed pyrolysis of cotton stalk for liquid and solid products, Fuel Process. Technol. 86 (2005) 1207–1219. https://doi.org/10.1016/j.fuproc.2004.12.006.

[29] J. lu Zheng, W. ming Yi, N. na Wang, Bio-oil production from cotton stalk, Energy Convers. Manag. 49 (2008) 1724–1730. https://doi.org/10.1016/j.enconman.2007.11.005.

[30] Z. Fang, R.L. Smith, L. Xu, Production of Biofuels and Chemicals with Pyrolysis, 2015. http://link.springer.com/10.1007/978-94-017-9612-5.

[31] N.U. Hasan, M.M. Rahman, R.I. Rahat, Characteristics comparison of pyrolysed oils obtained from waste of plastic, tyres and biomass solid, 4th Int. Conf. Adv. Electr. Eng. ICAEE 2017. 2018-Janua (2017) 450–454. https://doi.org/10.1109/ICAEE.2017.8255398.

[32] P. Madhu, H. Kanagasabapathy, I.N. Manickam, Conversion of cotton residues to bio-

oil and chemicals through flash pyrolysis in a fluidised bed reactor, Int. J. Energy Technol. Policy. 14 (2018) 20–33. https://doi.org/10.1504/IJETP.2018.088275.

[33] S. Adhikari, H. Nam, J.P. Chakraborty, Conversion of solid wastes to fuels and chemicals through pyrolysis, Elsevier B.V., 2018. https://doi.org/10.1016/B978-0-444-63992-9.00008-2.

[34] M. Waqas, A.S. Aburiazaiza, R. Miandad, M. Rehan, M.A. Barakat, A.S. Nizami, Development of biochar as fuel and catalyst in energy recovery technologies, J. Clean. Prod. 188 (2018) 477–488. https://doi.org/10.1016/j.jclepro.2018.04.017.

[35] R.K. Sharma, J.B. Wooten, V.L. Baliga, P.A. Martoglio-Smith, M.R. Hajaligol, Characterization of char from the pyrolysis of tobacco, J. Agric. Food Chem. 50 (2002) 771–783. https://doi.org/10.1021/jf0107398.

[36] S.P. Sohi, E. Krull, E. Lopez-Capel, R. Bol, A review of biochar and its use and function in soil, Adv. Agron. 105 (2010) 47–82. https://doi.org/10.1016/S0065-2113(10)05002-9.

List of Publication:

Journal:

1. S.B. Prajapati, A. Gautam, S. Gautam, Biomass and Bioenergy **Non-isothermal kinetic study by TGA analysis of printed circuit boards and cotton stalk**, Biomass and Bioenergy. 172 (2023) 106746. https://doi.org/10.1016/j.biombioe.2023.106746. (Impact Factor: 5.774) (SCIE & SCOPUS)

2. S.B. Prajapati, A. Gautam, S. Gautam, **Debromination and improved phenol content in fuel oil generated from co - pyrolysis of non - metallic PCB and biomass,** Biomass Convers. Biorefinery (2022). https://doi.org/10.1007/s13399-022-03139-z (Impact Factor: 4.050) (SCIE & SCOPUS)

3. S.B. Prajapati, A. Gautam, S. Gautam, **The Effect of Cotton Stalk Concentration on Morphology and Fixing Bromine Content in Char while Co-Pyrolysis with Non-Metal Fractions of PCB,** Biomass Convers. Biorefinery (2022) https://doi.org/10.1007/s13399-022-03515-9 (Impact Factor: 4.050) (SCIE & SCOPUS)

4. S. B. Prajapati, A. Gautam, S. Gautam, Z. Yao , F. Tesfaye, X. Lü, **Co-pyrolysis behaviour, kinetic and mechanism of waste printed circuit board with Biomass,** Processes, (2023) 1–21. https://doi.org/10.3390/pr11010229. (Impact Factor: 3.352) (SCIE & SCOPUS)

5. S.B. Prajapati, A. Gautam, S. Gautam, **Co-pyrolysis of PCB and cotton stalk: Towards enhanced phenol production and debromination of pyrolysis oil**, Chemical and Process Engineering 2022, 43 (2), 1–14. DOI: 10.24425/cpe.2022.140823. (Impact Factor: 0.679) (SCOPUS)

6. S. B. Prajapati, A. Gautam, S. Gautam, **Co-pyrolysis of PCB: Towards enhanced phenol production and debromination - Review,** Under Review

Conference Proceedings:

1. Sonal Prajapati, S. Gautam, **Co-pyrolysis of PCB with Cotton stalk: Product Characterization**, International Chemical Engineering Conference 2021, Organized by Department of Chemical Engineering Dr. B.R. Ambedkar National Institute of Technology, Jalandhar.

2. Sonal Prajapati, S. Gautam, **Pyrolysis of E-waste for Fuel oil Generation: A Review,** Schemcon (2019), 15th annual session of student's chemical engineering congress, Shroff S. R. Rotary Institute of Chemical technology, Ankleshwar.